https://doi.org/10.22226/2410-3535-2021-4-386-391 PACS: 72.80.Tm, 81.20.-n, 81.20.Ka

Spectroscopic study of Co-doped $CaCu_3Ti_4O_{12}$

N. A. Zhuk[†,1], E. U. Ipatova[2], B. A. Makeev[3], S. V. Nekipelov[4], A. V. Koroleva[5], L. A. Koksharova[1], R. I. Korolev[1]

[†]nzhuck@mail.ru

[1]Syktyvkar State University, Syktyvkar, 167001, Russia
[2]Institute of Chemistry of the Komi Science Center UB RAS, Syktyvkar, 167982, Russia
[3]Institute of Geology of the Komi Science Center UB RAS, Syktyvkar, 167982, Russia
[4]Institute of Physics and Mathematics of the Komi Science Center UB RAS, Syktyvkar, 167982, Russia
[5]Saint Petersburg State University, St. Petersburg, 198504, Russia

Calcium-copper titanate has been thoroughly studied by scientists around the world for several decades due to the manifestation of colossal dielectric permeability values ($\varepsilon \sim 10^4 - 10^5$) in wide frequency ranges ($10^2 - 10^6$ Hz) and temperature ranges (100 – 600 K), showing neither ferroelectric nor relaxor properties. Due to the unique dielectric characteristics of calcium-copper titanate (CCTO), materials based on it are promising for the manufacture of multilayer capacitors and microwave devices. Restrictions on the practical use of CCTO are caused by high dielectric losses. Electrophysical characteristics are optimized by modifying the CCTO composition, partially replacing copper, titanium and calcium cations. Good dielectric properties are demonstrated by the CCTO ceramics doped with cobalt atoms. Co-doped $CaCu_3Ti_4O_{12}$ was obtained by solid phase synthesis method. The samples are characterized by a grain microstructure; a thin layer of CuO is fixed in the intergranular space. From the interpretation of the obtained XPS- and NEXAFS 2p-spectra of Co-doped $CaCu_3Ti_4O_{12}$ and the corresponding oxides it can be concluded that in the Co-doped CCTO atoms of copper and calcium have a charge state of +2, atoms of titanium — $+(4-\delta)$, and cobalt atoms mainly +2 with some fraction of Co (III) in the high spin state. The Co-doped sample FTIR spectrum clearly captures the absorption bands in the fingerprint area at ≈408, 488, 539 cm^{-1}, which are typical for CCTO.

Keywords: cobalt, calcium-copper titanate, XPS, NEXAFS and FTIR spectroscopy.

УДК: 537.3, 537.9, 538.9

Спектроскопическое исследование допированного кобальтом $CaCu_3Ti_4O_{12}$

Жук Н. А.[†,1], Ипатова Е. У.[2], Макеев Б. А.[3], Некипелов С. В.[4], Королева А. В.[5], Кокшарова Л. А.[1], Королев Р. И.[1]

[1]Сыктывкарский государственный университет, Сыктывкар, 167001, Россия
[2]Институт химии Коми НЦ УрО РАН, Сыктывкар, 167982, Россия
[3]Институт геологии Коми НЦ УрО РАН, Сыктывкар, 167982, Россия
[4]Институт физики и математики Коми НЦ УрО РАН, Сыктывкар, 167982, Россия
[5]Санкт-Петербургский государственный университет, С.-Петербург, 198504, Россия

Титанат кальция-меди тщательно изучается учеными всего мира на протяжении нескольких десятилетий в связи с проявлением колоссальных значений диэлектрической проницаемости ($\varepsilon \sim 10^4 - 10^5$) в широком частотном ($10^2 - 10^6$ Гц) и температурном диапазонах (100 – 600 К). Благодаря уникальным диэлектрическим характеристикам титаната кальция-меди (CCTO) материалы на его основе перспективны для изготовления многослойных конденсаторов и устройств СВЧ. Ограничения на практическое использование обусловлены высокими диэлектрическими потерями CCTO. Электрофизические характеристики оптимизируются за счет изменения состава титаната кальция-меди, частичной замены катионов меди, титана и кальция. Хорошие диэлектрические свойства демонстрирует керамика

ССТО, легированная атомами кобальта. В данной работе мы представляем результаты исследований электронного состояния атомов в ССТО, легированного кобальтом, методами XPS, NEXAFS, а также ИК - Фурье спектроскопии. Co-легированный $CaCu_3Ti_4O_{12}$ получен методом твердофазного синтеза. Образцы характеризуются зеренной микроструктурой; в межзеренном пространстве различим тонкий слой CuO. Из интерпретации XPS- и NEXAFS 2p-спектров $CaCu_3Ti_4O_{12}$, легированного кобальтом, и соответствующих оксидов, пришли к выводу, что ионы меди и кальция имеют зарядовое состояние +2, ионы титана $+(4-\delta)$, а ионы кобальта, в основном, +2 с некоторой долей Co (III) в высокоспиновом состоянии. В ИК спектре образца, легированного кобальтом, фиксируются полосы поглощения в области отпечатков пальцев при 408, 488, 539 $см^{-1}$, характерные для титаната кальция- меди.

Ключевые слова: кобальт, титанат кальция-меди, XPS, NEXAFS и ИК-спектроскопия.

1. Introduction

Calcium-copper titanate has been thoroughly studied by scientists around the world for several decades due to the manifestation of colossal dielectric permeability values ($\varepsilon \sim 10^4 - 10^5$) in wide frequency ranges ($10^2 - 10^6$ Hz) and temperature ranges (100 – 600 K), showing neither ferroelectric nor relaxor properties [1–3]. A great number of researches are devoted to finding out the reasons of the abnormal behavior of calcium-copper titanate and its related compounds. The most probable model for describing the unique properties of calcium-copper titanate is the model of the internal barrier layer capacity (IBLC). It is based on the assumption of the heterogeneous composition of CCTO ceramics, in which the stoichiometry and electrical properties of micro-grain boundaries differ significantly from the properties of internal non-conductive areas [4, 5]. Meanwhile, the giant dielectric responses observed in CCTO single crystals without grain boundaries indicate that the cause is in other internal effects [6]. It is believed that oxygen deficiency in CCTO is compensated by the low-value Ti^{3+} and Cu^{+} ions present in ceramics [7]. The mixed valence structure Cu^{+}/Cu^{2+} and Ti^{3+}/Ti^{4+}, correlated with oxygen vacancies, can be an internal mechanism of the giant dielectric response of CCTO [6, 7]. Confirmation of the presence of ions Ti^{3+} and Cu^{+} was mainly obtained from the interpretation of XPS spectra CCTO [6 – 9]. Meanwhile, a NEXAFS-study of undoped CCTO and Ni-doped CCTO did not give confirmation of this; in the spectra are not shown low-valence ions [10,11]. The origin of the giant dielectric behavior of CCTO remains controversial.

Due to the unique dielectric characteristics of calcium-copper titanate (CCTO), materials based on it are promising for the manufacture of multilayer capacitors and microwave devices. Restrictions on the practical use of CCTO are caused by high dielectric losses [12]. Electrophysical characteristics are optimized by modifying the CCTO composition [13,14]. Good dielectric properties are demonstrated by the CCTO ceramics doped with cobalt atoms [15–18]. For example, $CaCu_{3-x}Co_xTi_4O_{12}$ films demonstrate good dielectric frequency stability, $e \approx 3143 - 3146$ and low tan $\delta \approx 0.016 - 0.017$ [16]. Improved dielectric properties are observed in a sample with a Co 5% alloy ($CaCu_{3-x}Co_xTi_4O_{12}$): $e \approx 7.4 \times 10^4$ and dielectric losses tan $\delta \approx 0.034$ at room temperature and 1 kHz. The low dielectric losses of CCTO were due to high intergranular resistance and increased dosing vacancy rates [17]. It is shown that with increasing cobalt content, the proportion of Co (III) increases, which is distributed in position Ti (IV). Cobalt cations are mainly located in the copper position that is shown in [19] C. Mu et al [20]. concluded that cobalt may exist in the states +2 and +3 and may take positions of Cu^{2+} and Ti^{4+}, depending on its degree of oxidation. An increase in dielectric permeability and other low-frequency relaxation due to the presence of an impurity phase is observed in $CaCu_3Ti_{3.8}Co_{0.2}O_{12}$. However, Fang et al [21] have found that the dielectric response of CCTO doped with cobalt is exactly the same as that of CCTO. The ceramic $CaCu_{2.8}Co_{0.2}Ti_4O_{12}$ exhibits high dielectric permeability values ($e_r = 25400$ synthesized at 1000°C and e_r=111000 (at 1050°C)) at low frequencies (50 Hz) is shown in [22].

This paper presents the results of studies of the electron state of atoms in Co-doped CCTO using XPS, NEXAFS methods, and FTIR spectroscopy..

2. Materials and methods

The solid solution samples ($CaCu_3Ti_{4-4x}Co_{4x}O_{12-\delta}$, $x \le 0.06$) were obtained via the standard ceramic procedure from "special pure" grade $CaCO_3$ and Co (II), Ti (IV), Cu (II) oxides using staged calcination at 650, 850, 950 and 1050°C for 50 hours. The phase composition of the studied samples was controlled by X-ray phase analysis (DRON-4-13, $Cu_{K\alpha}$-radiation) and scanning electron microscopy (a scanning electron microscope Tescan MIRA 3LMN, an energy dispersive spectrometer INCA Energy 450), the unit cell parameters of the solid solutions were calculated using the CSD software package [23].

Fourier transform infrared (FTIR) spectra were recorded on a IRPrestige-21 Shimadzu (Japan) spectrophotometer equipped with a DLATGS detector in the wavenumber range of 400 – 4000 $см^{-1}$ with a resolution of 4 $см^{-1}$. Before analysis, the samples were mixed and grinding with KBr (2% of a sample by weight). The transmission spectra were obtained using the diffuse reflection mode. The data were processed using Shimadzu software.

Samples of cobalt-doped calcium-copper titanate were studied by NEXAFS spectroscopy using synchrotron radiation from a BESSY II Storage Ring (Berlin, Germany). NEXAFS spectra were obtained by recording the total electron yield (Total electron yield, TEY) [24].

XPS-research was carried out using the equipment of the resource center of the Scientific Park of St. Petersburg State University "Physical methods of surface investigation". XPS-analysis was carried out on a Thermo Scientific ESCALAB 250Xi X-ray spectrometer. An X-ray tube with $Al_{K\alpha}$ radiation (1486.6 eV) was used as an ionizing radiation source. To neutralize the charge of the sample in the experiments the ion-electronic charge compensation system was used. All

peaks were calibrated relative to the C1s peak at 284.6 eV. The processing of experimental data was carried out using the software of the ESCALAB 250 Xi spectrometer.

3. Results and discussion

3.1. Phase composition and microstructure of samples

Ceramic preparations of $CaCu_3Ti_{4-4x}Co_{4x}O_{12-\delta}$ were studied in a limited concentration range at $x \leq 0.06$. It was established by X-ray phase analysis (Fig. S1, Supplementary material) that Co-doped CCTO crystallizes in the structural type of double perovskite (sp. gr. *Im3*). The X-ray analysis of the samples show hardly visible reflexes of copper oxide (II), which is confirmed by the data of scanning electron microscopy.

As a result of calculating the parameters of the solid solutions cell it was established that for the samples of $CaCu_3Ti_{4-4x}Co_{4x}O_{12-\delta}$ the parameter is close to the parameter of calcium-copper titanate, showing a tendency to increase: from 0.73926 nm ($x=0.01$) to 0.73962 nm ($x=0.06$) ($R(Co(III))_{c.n=6(h.s.)}$=0.0545 nm; $R(Co(III))_{c.n=6(l.s)}$=0.061 nm; $R(Co(II))_{c.n=6(h.s.)}$=0.065 nm; $R(Co(II))_{c.n=6(l.s)}$=0.0745 nm)) [25]. Pictures of crystalline powders of the synthesized preparations are shown in the Fig. S2 (Supplementary material).

The dissolution of cobalt oxide in the ceramics of calcium-copper titanate is confirmed by the data of EDS spectra and microprobe analysis (Fig. S2, Supplementary material). As can be seen from microphotographs, samples are characterized by a grain microstructure; the sizes of rounded, slightly melted grains vary in the range of 2–10 μm. In microphotographs, copper oxide (II), distributed in the intergranular space, as a layer between the grains of ceramics, is clearly visible. Apparently, the presence of impurities copper oxide (II) in ceramics is caused not only by the partial distribution of cobalt (II) ions in the copper (II) position, but also by the thermal dissociation of $CaCu_3Ti_{4-4x}Co_{4x}O_{12-\delta}$ [26], which can be evidenced by the rounded shape of ceramic grains and a thin uniform copper oxide layer, typical for the cooled melt.

3.2. NEXAFS, XPS and FTIR spectroscopy

To determine the charge state of cobalt atoms, the samples were examined by NEXAFS-spectroscopy using a BESSY-II synchrotron source. All NEXAFS spectra (Fig. 1a–d) were recorded in total electron yield (TEY) [24]. Fig. 1d shows the absorption spectra of cobalt atoms in CCTO and the Co_3O_4 and CoO spectra [27]. As can be seen, the cobalt spectra in calcium-copper titanate are the closest in intensity and energy position to the main peaks with the corresponding details of $Co2p_{3/2}$ CoO spectra and are less similar to the Co_3O_4 spectra. Cobalt atoms in CoO are bivalent, i.e. they have the charge state of Co^{2+}, while in mixed Co_3O_4 oxide cobalt atoms are present in the oxidation degrees (II) and (III). It should be noted that the cobalt spectrum in Co_3O_4 can be considered as a superposition of the cobalt spectra in the charge state of Co^{2}+ and Co^{3}+, with a more intense peak in the region of 782 eV being responsible for the Co^{3+} contribution, and a low-energy band (779–780 eV) for the Co^{2+} contribution, which correlates well with the CoO spectra.

When looking at the spectra in detail, the following differences can be seen. The absorption line component at 779 eV in $CaCu_3Ti_{4-4x}Co_{4x}O_{12-\delta}$ is strongly blurred in contrast to the CoO spectrum; the intensity ratio of the spectrum components at 781 and 779.5 eV in the $CaCu_3Ti_{4-4x}Co_{4x}O_{12-\delta}$

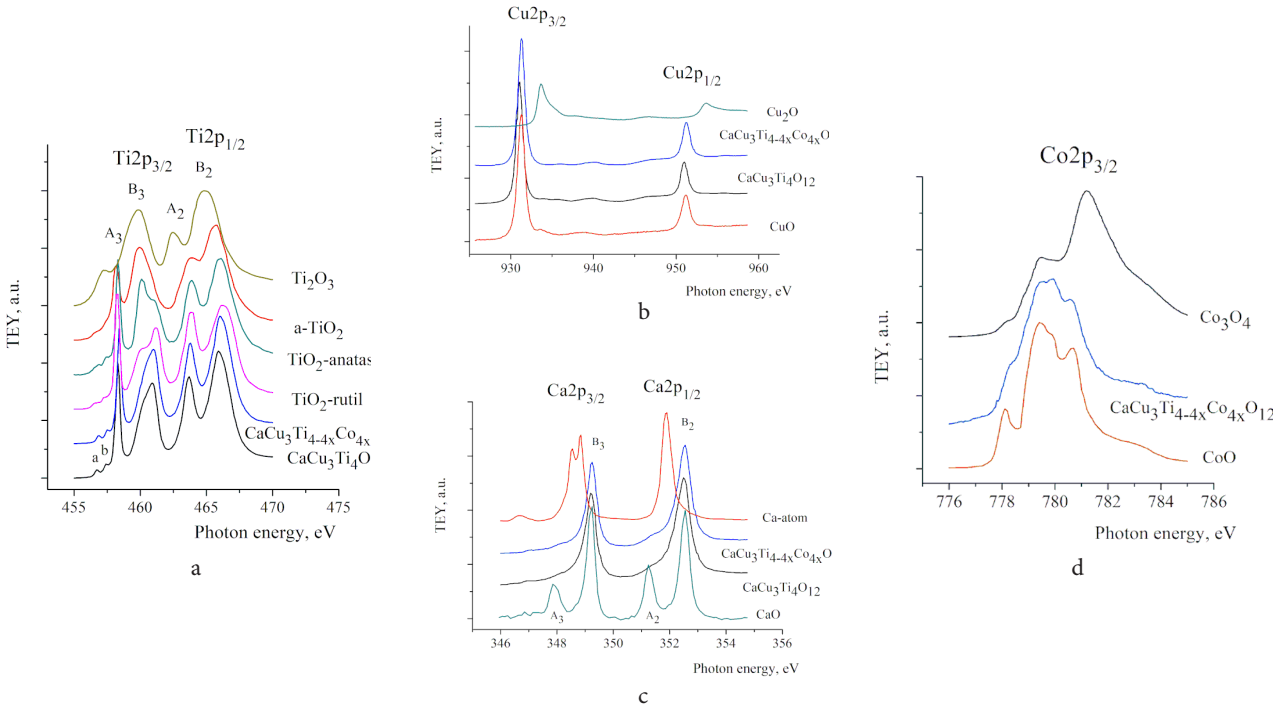

Fig. 1. (Color online) NEXAFS Ti2p-spectra of the $CaCu_3Ti_{4-4x}Co_{4x}O_{12-\delta}$ and titanium oxides (a); NEXAFS Cu2p- spectra of the $CaCu_3Ti_{4-4x}Co_{4x}O_{12-\delta}$ and copper oxides (b); NEXAFS Ca2p-spectra of calcium in $CaCu_3Ti_{4-4x}Co_{4x}O_{12-\delta}$, CaO and atomical calcium (c); NEXAFS Co2p- spectra of the $CaCu_3Ti_{4-4x}Co_{4x}O_{12-\delta}$ and cobalt oxides (d).

spectrum is slightly lower than for CoO and, in general, the $CaCu_3Ti_{4-4x}Co_{4x}O_{12-\delta}$ spectrum is wider and diffuse in comparison with the cobalt oxide (II) spectrum. This suggests that the Co-doped CCTO spectrum is a superposition of the Co (II) and Co (III), with less content of the latter. If we compare the calculated spectra for the octahedron-coordinated cobalt ions given in [28, 29] and obtained by us, it is most likely that the high spin Co (III) ion replacing the Ti (IV) position will take place in the form of the Co2p spectrum for $CaCu_3Ti_{4-4x}Co_{4x}O_{12-\delta}$ and its energy position.

NEXAFS-spectra of titanium, calcium and copper ions in $CaCu_3Ti_{4-4x}Co_{4x}O_{12-\delta}$ and oxide spectra are shown in the Fig. 1a – c. NEXAFS-spectra of titanium, calcium and copper ions in $CaCu_3Ti_{4-4x}Co_{4x}O_{12-\delta}$ are discussed in detail in [10,11]. It remains to emphasize that doping with cobalt does not change the main characteristics of their spectra. This allows us to interpret spectral characteristics of atoms of calcium, copper and titanium in a similar way. In particular, from the interpretation of the obtained NEXAFS 2p spectra, it can be concluded that in the considered CCTO compounds the copper and calcium atoms have the charge state +2, the titanium atoms — +(4 – δ).

In order to clarify the charge state in the Co-doped CCTO researches by XPS-spectroscopy method (Fig. 2) were conducted.

For comparison, the CCTO spectra obtained and interpreted by us earlier [11], as well as spectra of CoO [27] and Co_3O_4 oxides are presented. When considering the obtained spectra, we can conclude that in the considered CCTO compounds copper and calcium atoms have a charge +2, which coincides with the results of the analysis of NEXAFS spectra conducted above. As for titanium atoms, in spite of the fact that their XPS spectra in CCTO and Co-doped CCTO have almost complete similarity with TiO_2 spectra both in form and in mutual arrangement of the main parts, it is necessary to note the energy shift ≈0.8 eV towards lower energies, which manifests itself at reduction of effective positive charge [10,11,31]. This allows us to conclude that titanium atoms in the Co-doped CCTO have the same effective charge +(4 – δ), i. e., are in equivalent positions in the CCTO.

XPS spectra of cobalt atom absorption are shown in Fig. 2e. Spectra of CoO [27] and Co_3O_4 oxides are given for comparison. The energy position of the main peaks in all three given spectra is practically the same (Table S1, Supplementary material). Thus, in spectra of CCTO and CoO there are strongly expressed satellite peaks that is characteristic feature practically for all XPS 2p-spectra of 3d atoms in divalent state [32].

This confirms the above conclusion based on the analysis of NEXAFS spectra, that doped cobalt atoms in the CCTO mainly have the charge state +2. It may be noted that the main peaks of Co2p-spectra have the stretched high-energy ending, which the authors [15, 22] interpret as the presence of Co (III). With this in mind, our findings correlate with the results of the study of CCTO samples doped with cobalt atoms prepared both by the traditional sintering method [17,19] and for thin sprayed films [15,16]. At the same time, it can be noted that in [15 –19] studied samples of $CaCu_{3-x}Ti_4Co_xO_{12}$, and it is concluded that cobalt atoms are introduced into the copper position. In [19] it is noted that the introduction of cobalt atoms in the copper position is typical only for small concentrations of the drug (up to $x = 0.05$), and at higher values of the index x it is possible to introduce cobalt atoms in both copper and titanium positions.

From the interpretation of the obtained XPS and NEXAFS 2p-spectra, it can be concluded that in the Co-doping CCTO atoms of copper and calcium have a charge state of +2, atoms of titanium — +(4 – δ), and cobalt atoms mainly +2 with some fraction of Co (III), probably in the high spin state.

The samples of the Co-doped CCTO, CCTO and CoO were characterized by using infrared spectra with Fourier

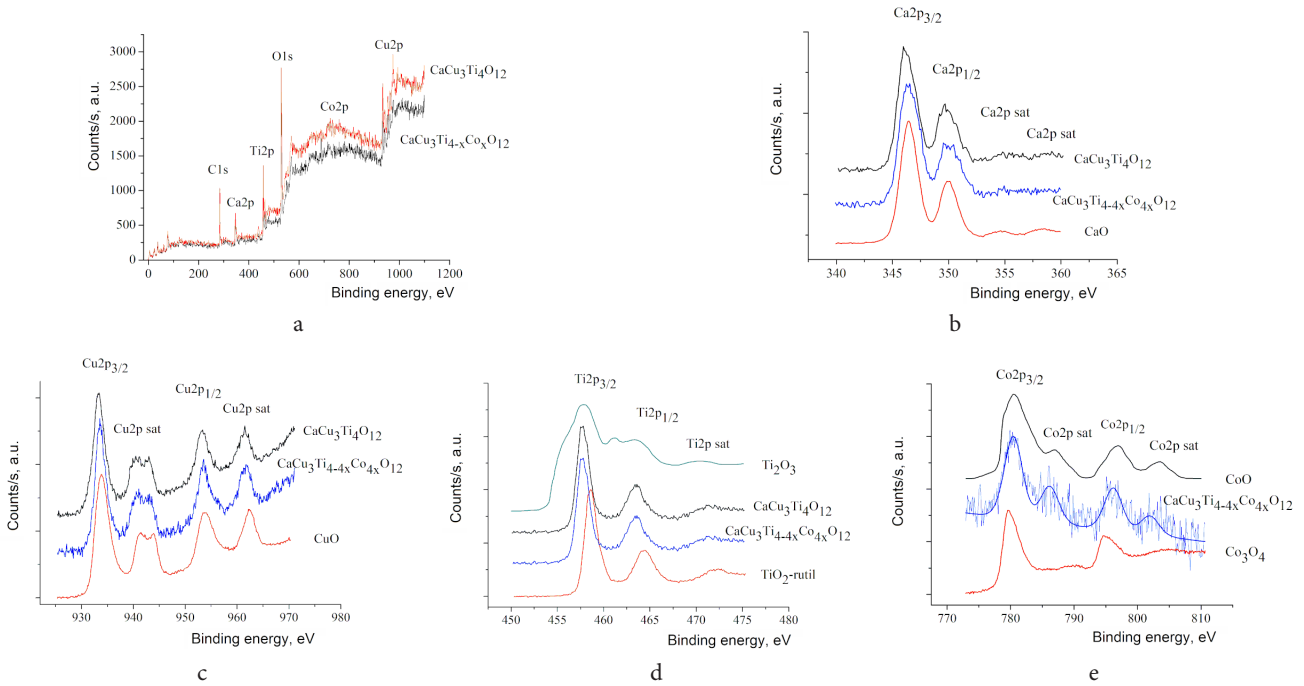

Fig. 2. (Color online) XPS-spectra of calcium (b), copper (c), titanium (d), cobalt (e) and survey-spectra (a) in the $CaCu_3Ti_{4-4x}Co_{4x}O_{12-\delta}$.

transform. The FTIR spectra of the samples are recorded in a matrix of potassium bromide in the frequency range of 400 – 4000 cm^{-1} (Fig. S3, Supplementary material).

The figure shows fragments of FTIR spectra of three samples of the $CaCu_3Ti_{4-4x}Co_{4x}O_{12-\delta}$ ($x = 0.06$), CoO, $CaCu_3Ti_4O_{12}$ composition. The attribution of the observed absorbance bands is based on the literature data [33 – 38], and the Co-doped CCTO are reproduced with the data given in the literature. Three absorption bands in the fingerprint region at ≈408, 488, 539 cm^{-1} are clearly recorded on the spectra of CCTO samples, associated according to the data [33] with valence oscillations of TiOTi (410), Cu-O (≈489) and Ca-O bonds at 540 cm^{-1} in CCTO. The authors [34, 35] connect the absorption bands at 540 and 489 cm^{-1} with the valence oscillations of TiO bond in the octahedron TiO_6. The wide diffuse absorption band in the region of 600 –1200 cm^{-1}, typical for CCTO and Ni, Co-doped CCTO, observed earlier in works [36, 37], attracts attention. On its background, the maximums at 1094 –1105, 802 – 860 cm^{-1}, which can be associated with vibrations of CuO_4, TiO_6 groups, are clearly seen [37]. In the spectral area of 400 – 600 cm^{-1} valence oscillations of Co-O appear. According to the literature, at 548 – 570 cm^{-1} the absorption band of valence oscillations of Co (III)-O bond is fixed in the octahedron CoO_6 [38], and in the region 653 – 663 cm^{-1} the band is responsible for oscillations of Co (II)-O bond in the tetrahedron CoO_4. In the spectrum of compounds, the frequency range of 400 – 600 cm^{-1} is overlapping with the characteristic CCTO absorption bands; therefore, Co (II)-O oscillations on their background are not reliably identified. However, when comparing the CoO and Co-doped CCTO spectra, the absorption band in the ≈681 cm^{-1} and 702 – 716 cm^{-1} range is observed, the presence of which indirectly indicates the presence of Co (II) atoms in the structure of solid solutions.

4. Conclusions

Samples of $CaCu_3Ti_{4-4x}Co_{4x}O_{12-\delta}$ ($x \le 0.06$) were synthesized using standard ceramic technology. According to XRD analysis data, copper oxide (II) reflexes are fixed as an impurity phase in trace amounts. Copper oxide (II) is distributed in intergranular space as a uniform thin layer. From the interpretation of the obtained XPS- and NEXAFS 2p-spectra of atoms in the Co-doped $CaCu_3Ti_4O_{12}$ and the corresponding oxides it was concluded that in ceramics the copper and calcium atoms have a charge state of +2, the titanium atoms have a slightly lower charge than +4, and cobalt atoms have mainly a charge of +2 with some fraction of Co (III) ions in the high spin state. The Co-doped CCTO sample spectrum clearly captures the characteristic absorption bands in the fingerprint area at ≈408, 488, 539 cm^{-1} associated with valence oscillations of TiO, TiOTi, Cu-O and Ca-O bonds. Against their background, the absorption bands of the valence oscillations of the CaO bond are not identified satisfactorily.

Supplementary material. *The online version of this paper contains supplementary material available free of charge at the journal's Web site (lettersonmaterials.com).*

Acknowledgment. The authors acknowledge the Research Center "Physical methods of surface investigation" of the Scientific Park of St. Petersburg University.

References

1. A. Deschanvres, B. Raveau, F. Tollemer. Bull. Soc. Chim. Fr. 15, 4077 (1967).
2. M. A. Subramanian, D. Li, N. Duan, B. A. Reisner, A. W. Sleight. J. Sol. St. Chem. 151, 323 (2000). Crossref
3. J. Li, A. W. Sleight, M. A. Subramanian. Sol. St. Commun. 135, 260 (2005). Crossref
4. S. Krohns, P. Lunkenheimer, S. G. Ebbinghaus, A. Loidl. J. Appl. Phys. 103, 084107 (2008). Crossref
5. J. J. Mohamed, S. D. Hutagalung, M. F. Ain, K. Deraman, Z. A. Ahmad. Mater. Lett. 61, 1835 (2007). Crossref
6. L. Ni, X. M. Chen. Appl. Phys. Lett. 91, 122905 (2007). Crossref
7. L. Ni, X. M. Chen. J. Am. Ceram. Soc. 93,184 (2010). Crossref
8. C. Wang, H. J. Zhang, P. M. He, G. H. Cao. Appl. Phys. Lett. 91, 052910 (2007). Crossref
9. G. Deng, N. Xanthopoulos, P. Muralt. Appl. Phys. Lett. 92, 172909 (2008). Crossref
10. N. A. Zhuk, S. V. Nekipelov, V. N. Sivkov, B. A. Makeev, R. I. Korolev, V. A. Belyy, M. G. Krzhizhanovskaya, M. M. Ignatova. Mater. Chem. Phys. 252, 123310 (2020). Crossref
11. N. A. Zhuk, S. V. Nekipelov, V. N. Sivkov, N. A. Sekushin, V. P. Lutoev, B. A. Makeev et al. Ceram. Intern. 46, 21410 (2020). Crossref
12. M. Ahmadipour, M. F. Ain, Z. A. Ahmad. Nano-Micro Letters. 8, 291 (2016). Crossref
13. F. Amaral, E. Clemente, M. A. Valente, L. C. Costa, F. M. Costa. Ceram. Intern. 40, 16503 (2014). Crossref
14. M. Li, Q. Liu, C. X. Li. J. Alloy Comp. 699, 278 (2017). Crossref
15. D. Xu, X. Yue, Y. Zhang, J. Song, X. Chen, S. Zhong, J. Ma, L. Ba, L. Zhang, S. Du. J. Alloys Comp. 773, 853 (2019). Crossref
16. X. Yue, W. Long, J. Liu, S. Pandey, S. Zhong, L. Zhang, et. al. J. Alloys Comp. 816, 152582 (2020). Crossref
17. J. Wang, Z. Lu, T. Deng, C. Zhong, Z. Chen. J. Eur. Ceram. Soc. 38, 3505 (2018). Crossref
18. K. D. Mandal, A. K. Rai, L. Singh, O. Parkash. Bull. Mater. Sci. 35, 433 (2012). Crossref
19. S.-Y. Chung, S.-Y. Choi, T. Yamamoto, Y. Ikuhara, S.-J. L. Kang. Appl. Phys. Lett. 88, 091917 (2006). Crossref
20. C. Mu, Y. Song, H. Wang, X. Wang. J. Appl. Phys. 117, 17B723 (2015). Crossref
21. L. Fang, M. Shen, F. Zheng, Z. Li, J. Yang. J. Appl. Phys. 104, 064110 (2008). Crossref
22. S. Jesurani, S. Kanagesan, K. Ashok. J. Sol-Gel Sci. Techn. 64, 335 (2012). Crossref
23. L. G. Akselrud, Yu. N. Grin, P. Yu. Zavalii, V. K. Pecharski, V. S. Fundamentski. Twelfth European Crystallogr. Meeting, Collected Abstracts. Moscow (1989) p. 155.
24. J. Stohr. NEXAFS Spectroscopy. Springer. Berlin (1992). Crossref
25. R. D. Shannon. Acta Crystallogr. A. 32, 751 (1976). Crossref

26. N. A. Zhuk, S. M. Shugurov, V. A. Belyy, B. A. Makeev, M. V. Yermolina, D. S. Beznosikov, L. A. Koksharova. Ceram. Intern. 44, 20841 (2018). Crossref
27. T. J. Regan, H. Ohldag, C. Stamm, F. Nolting, J. Luning, J. Stöhr, R. L. White. Phys. Rev. B. 64, 214422 (2001). Crossref
28. S. Y. Istomin, O. A. Tyablikov, S. M. Kazakov, E. V. Antipov, A. I. Kurbakov, A. A. Tsirlin, N. Hollmann, Y. Y. Chin, H.-J. Lin, C. T. Chen, A. Tanaka, L. H. Tjeng, Z. Hu. Dalt Trans. 44, 10708 (2015). Crossref
29. M. Merz, D. Fuchs, A. Assmann, S. Uebe, H. V. Lohneysen, P. Nagel, S. Schuppler. Phys. Rev. B. 84, 014436 (2011). Crossref
30. S. O. Kucheyev, T. van Buuren, T. F. Baumann, J. H. Satcher, Jr. T. M. Willey, R. W. Meulenberg, T. E. Felter, J. F. Poco, S. A. Gammon, L. J. Terminello. Phys. Rev. B. 69, 245102 (2004). Crossref
31. M. Hassel, H.-J. Freund. Surface Science Spectra. 4, 273 (1996). Crossref
32. J. F. Moulder. Handbook of X-ray Photoelectron Spectroscopy: A Reference Book of Standard Spectra for Identification and Interpretation of XPS Data. Physical Electronics Division, Perkin-Elmer Corporation (1992) 261 p.
33. S. Jesurani, S. Kanagesan, R. Velmurugan, T. Kalaivani. J. Mater. Sci.: Mater. Electron. 23, 668 (2011).
34. N. Hadi, A. Farid, T.-E. Lamcharfi, A. Belaaraj, S. Kassou, F. Ahjyaje. J. Chem. 8, 245 (2019).
35. L. C. Kretly, A. F. L. Almeida, P. B. A. Fechine, R. S. de Oliveira, A. S. B. Sombra. J. Mater. Sci. Mater. Electron. 15, 657 (2004). Crossref
36. C. Masingboon, S. Maensiri, T. Yamwong, P. L. Anderson, S. Seraphin. Appl. Phys. A. 91, 87 (2007). Crossref
37. A. F. L. Almeida, P. B. A. Fechine, M. P. F. Graça, M. A. Valente, A. S. B. Sombra. J. Mater. Sci.: Mater. Electron. 20, 163 (2008).
38. M. Premila, A. Bharathi, N. Gayathri, P. Yasodha, Y. Hariharan, C. S. Sundar. J. Phys. 67, 153 (2006).